SEMARAK ILMU PUBLISHING

Journal of Advanced Research in Numerical Heat Transfer

Journal homepage:
https://semarakilmu.com.my/journals/index.php/arnht/index
ISSN: 2735-0142

Thermogravitational Convection in a Controlled Rotating Darcy-Brinkman Nanofluids Layer Saturated in an Anisotropic Porous Medium Subjected to Internal Heat Source

Izzati Khalidah Khalid[1,*], Nor Fadzillah Mohd Mokhtar[2], Nurul Hafizah Zainal Abidin[3]

[1] School of Mathematical Sciences, College of Computing, Informatics and Media, Universiti Teknologi MARA, UiTM Shah Alam, 40450 Shah Alam, Selangor Darul Ehsan, Malaysia
[2] Department of Mathematics, Faculty of Science, Universiti Putra Malaysia, 43400 Serdang, Selangor Darul Ehsan, Malaysia
[3] Mathematical Sciences Studies, College of Computing, Informatics and Media, Universiti Teknologi MARA, Perak Branch, Tapah Campus, 35400 Tapah Road, Perak Darul Ridzuan, Malaysia

ARTICLE INFO

Article history:
Received 18 June 2023
Received in revised form 15 July 2023
Accepted 19 August 2023
Available online 30 September 2023

Keywords:
Darcy-Brinkman model; Thermogravitational Convection; Nanofluids Layer; Rotation; Porous Medium; Feedback Control

ABSTRACT

Thermogravitational convection in a controlled rotating Darcy-Brinkman nanofluids layer saturated in an anisotropic porous medium heated from below is investigated. The presence of a uniformly distributed internal heat source and considers the Brinkman model for different boundary conditions: rigid-rigid, free-free, and lower-rigid and upper-free are considered. The effect of a control strategy involving sensors located at the top plate and actuators positioned at the bottom plate of the nanofluids layer is analysed. Linear stability analysis based on normal mode technique is employed. The resulting eigenvalue problem is solved numerically using the Galerkin method implemented with Maple software. The model used for the nanofluids associates with the mechanisms of Brownian motion and thermophoresis. The influences of the internal heat source strength, mechanical anisotropy parameter, modified diffusivity ratio, nanoparticles concentration Darcy-Rayleigh number and nanofluids Lewis number are found to advance the onset of convection. Conversely, the Darcy number, thermal anisotropy parameter, porosity, rotation, and controller effects are observed to slow down the process of convective instability.

1. Introduction

Nanofluids are liquids containing nanoparticles, offer improved convective heat transfer and thermal conductivity properties to the fluids [1]. The Darcy-Benard problems of nanofluids layer involve the investigation of natural convection within a nanofluid layer bounded by two infinite parallel planes. These problems have garnered significant attention in numerous scientific, engineering, technological, chemical, nuclear, and biomechanical literature reviews due to their relevance [2-7]. The Darcy-Brinkman convective instability in nanofluids layer saturated within porous media focuses on studying the instability that arises from the interaction between fluid flow

* *Corresponding author.*
E-mail address: izzatikk@uitm.edu.my (Izzati Khalidah Khalid)

https://doi.org/10.37934/arnht.14.1.7090

and the resistance of the porous medium within a nanofluid layer. Yadav *et al.,* [6] conducted research on the effect of internal heat source in nanofluids layer saturated in porous media. Shivakumara *et al.,* [8] studied penetrative Brinkman convection in nanofluids layer saturated in an anisotropic porous medium. The Darcy-Brinkman equation is an appropriate model for fluid flow with highly porous materials. Chand *et al.,* [9] investigated the effects of variable gravity on thermal instability in a horizontal layer of nanofluids saturated in an anisotropic Darcy porous medium.

The occurrence of thermal convection in rotating fluids saturated in porous layer heated from below has attracted both experimental and theoretical interest. This phenomenon is particularly relevant in geophysical and oceanic flows. The effect of rotation on convective instability is crucial, as it has been theoretically proven by several researchers [10-14]. The stabilizing effect of rotation on thermal convective instability in fluids saturated in a porous medium has also been investigated [15-21]. Many experts have validated the application of feedback control, both experimentally and theoretically, to stabilize thermal convection [22-25]. Furthermore, researchers have explored the inclusion of other relevant effects, such as feedback control in conjunction with buoyancy and surface-tension driven [26-28]. Additionally, the impact of internal heat generation has been extensively studied, considering various types of fluids [29-37]. In recent times, Khalid *et al.,* [38-40] interplayed the combination effect of rotation, magnetic field, internal heat source and feedback control on thermal instability in nanofluids layer subjected to various effects. Besides, Abidin *et al.,* [41] focused on binary fluid saturated in anisotropic porous medium problem with variable viscosity effect respectively.

Recently, these authors have undertaken a novel investigation in their study. Arasteh *et al.,* [42] employed Darcy-Brinkman-Forchheimer model with local thermal non-equilibrium model or two equations method to model the momentum and energy equations in porous medium, respectively. Toghraie *et al.,* [43] proposed a 3D numerical study of convective heat transfer through a micro concentric annulus governing non-uniform heat flux boundary conditions employing water-Al_2O_3 nanofluid, a two-phase mixture model. Lately, Artificial Neural Networks (ANNs) are widely used in many scientific and engineering fields. These networks have shown their potential in predicting the nonlinear or complex behaviours of systems. He *et al.,* [44] generated experimental data points of Zinc Oxide and Silver (50%-50%)/Water nanofluid and proposed an algorithm to calculate the best neuron number in the ANN. Afterwards, they calculated the performance and correlation coefficient for ANN. Boroomandpour *et al.,* [45] investigate a comprehensive experimental investigation of thermal conductivity of a ternary hybrid nanofluid containing MWCNTs-titania-zinc oxide/water-ethylene glycol (80:20) as well as binary and mono nanofluids. Yan *et al.,* [46] studied the rheological behaviour of MWCNTs-ZnO/Water-Ethylene glycol hybrid non-Newtonian nanofluid by using of an experimental investigation. Lakshmi and Rallabandi [47] analysed the effect of Hall current and thermal radiation on the MHD flow of an electrically conducting Casson nanofluid across a constantly extending surface in the presence of heat source/sink, Brownian motion, and thermophoresis.

The motivation of this research is to study thermogravitational convection in Darcy-Brinkman nanofluids layer saturated in a rotating anisotropic porous medium, considering the effects of feedback control and internal heat source. This study is extended from Yadav *et al.,* [6], where the effects of rotation, feedback control, and anisotropic parameters was introduced. Therefore, the eigenvalue solution is extracted numerically using linear stability analysis and the normal mode technique. The Galerkin method is employed, and the solution is computed using Maple software. The results are presented graphically and thoroughly discussed. This study's findings will contribute valuable insights into the behaviour of nanofluids layer in porous media and aid in optimizing heat transfer systems for various engineering applications. It is important to emphasize that the internal

heat source significantly alters the temperature distribution in nanofluids, consequently affecting the rate of particle deposition in nuclear reactors, electronic chips, and semiconductor wafers.

2. Methodology

The onset of convection in a horizontal layer of a porous medium saturated by nanofluids is studied analytically. The model used for the nanofluids incorporates the effects of Brownian motion and thermophoresis. For the porous medium, the Brinkman model is employed. Consider an infinite horizontal layer of incompressible rotating nanofluids saturated Brinkman anisotropic porous layer with feedback control and internal heat source confined between the planes $z^* \in [0, L]$ heated uniformly from below. The schematic diagram of the system considered here is shown in Figure 1 below. The continuity equation, momentum equation, energy equation and conservation of the nanoparticle equation are discussed in detail below.

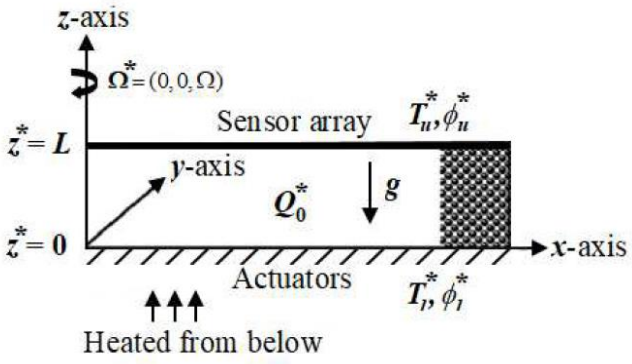

Fig. 1. Physical configuration and coordinate system

Considering the Brinkman model, the governing momentum equation in the presence of Coriolis force takes the form [3, 6]

$$\nabla^* \cdot \boldsymbol{u}_D^* = 0, \tag{1}$$

$$\frac{\rho_f \partial \boldsymbol{u}_D^*}{\varepsilon \partial t^*} = -\nabla^* p^* + \mu \nabla^{*2} \boldsymbol{u}_D^* - \mu \frac{\boldsymbol{u}_D^*}{K} - \frac{2\rho_f}{\varepsilon} \Omega^* \times \boldsymbol{u}_D^* + \boldsymbol{g}\left[\phi^* \rho_p + \left(1-\phi^*\right)\rho_f \left(1-\alpha_T\left[T^* - T_u^*\right]\right)\right], \tag{2}$$

$$\frac{(\rho c)_m \partial T^*}{\partial t^*} + (\rho c)_f \left(\boldsymbol{u}_D^* \cdot \nabla^*\right) T^* = \kappa_m \nabla^{*2} T^* + Q_0^* + \varepsilon (\rho c)_p \left[D_B \nabla^* \phi^* \cdot \nabla^* T^* + \left(\frac{D_T}{T_u^*}\right) \nabla^* T^* \cdot \nabla^* T^* \right], \tag{3}$$

$$\frac{\partial \phi^*}{\partial t^*} + \frac{\phi^*}{\varepsilon}\left(\boldsymbol{u}_D^* \cdot \nabla^*\right) = D_B \nabla^{*2} \phi^* + \frac{D_T}{T_u^*} \nabla^{*2} T^*, \tag{4}$$

Where $\boldsymbol{u}_D^* = \left(u^*, v^*, w^*\right)$ is the Darcy velocity, ρ_f is the density of the base fluid, ρ_p is the nanoparticle mass density, t^* is time, p^* is the pressure, μ is the viscosity, $\tilde{K}$ is the permeability of the porous medium, ε is the porosity of the porous medium, $\boldsymbol{g}$ is the gravitational force, ϕ^* is the nanoparticle volume fraction, α_T is the thermal volumetric coefficient, T^* is the temperature, $(\rho c)_m$ is the effective heat capacity, c is the specific heat, c_p is the specific heat of the nanoparticles, Q_0^* is the uniform internal heat source, $\tilde{\kappa}_m$ is the effective thermal conductivity of the porous medium

saturated by the nanofluid, D_B is the Brownian diffusion coefficient and D_T is the thermophoretic diffusion coefficient. The permeability and thermal conductivity tensors are defined as

$$\frac{1}{K}=\frac{1}{K_H}\left(\hat{i}\hat{i}+jj\right)+\frac{1}{K_V}kk, \tag{5}$$

$$\kappa_m=\kappa_{mH}\left(\hat{i}\hat{i}+jj\right)+\kappa_{mV}kk, \tag{6}$$

Where $\tilde{K}_H$ is the permeability and $\tilde{\kappa}_{mH}$ is the thermal conductivity in the horizontal $\hat{i}$ and j directions, while $\tilde{K}_V$ and $\tilde{\kappa}_{mV}$ are the corresponding values in the vertical k direction. It may be noted that horizontal mechanical and thermal isotropy has been assumed.

It assumes that the temperature and volumetric fraction of the nanoparticles are constant on the boundaries. Thus, the boundary conditions are:

$$w^*=0,\frac{\partial w^*}{\partial z^*}+\beta_1 L\frac{\partial^2 w^*}{\partial z^{*2}}=0,T^*=T_0^*,\phi^*=\phi_0^* \text{ at } z=0, \tag{7}$$

$$w^*=0,\frac{\partial w^*}{\partial z^*}-\beta_2 L\frac{\partial^2 w^*}{\partial z^{*2}}=0,T^*=T_1^*,\phi^*=\phi_1^* \text{ at } z=1. \tag{8}$$

Here, the parameters β_1 and β_2 each takes the value ∞ for the case of free boundary and 0 for a rigid boundary. To nondimensionalize the governing Eq. (1) – Eq. (4), the variables are scaled as follows:

$$\begin{aligned}&\left(x^*,y^*,z^*\right)=L\left(x,y,z\right),p^*=\frac{p\mu\kappa_v}{K_V},t^*=\frac{t\sigma L^2}{\kappa_v},\phi=\frac{\phi^*-\phi_l^*}{\phi_u^*-\phi_l^*},\psi_z^*=\frac{\psi_z\kappa_v}{L},t^*=\frac{t\sigma L^2}{\kappa_v},\\&\left(u^*,v^*,w^*\right)=\frac{\kappa_v}{L}\left(u,v,w\right),T=\frac{T^*-T_u^*}{\Delta T^*},\end{aligned} \tag{9}$$

Where $\kappa_v=\frac{\kappa_m}{\left(\rho c\right)_f}$ is the effective thermal diffusivity and $\sigma=\frac{\left(\rho c\right)_m}{\left(\rho c\right)_f}$ is the heat capacity ratio respectively. Substituting Eq. (9) into Eq. (1) – Eq. (4), we obtain:

$$\nabla\cdot\boldsymbol{u}_D=0, \tag{10}$$

$$\frac{Da}{\Pr}\frac{\partial\boldsymbol{u}_D}{\partial t}=-\nabla p+Da\nabla^2\boldsymbol{u}_D-\boldsymbol{u}_a-Rm\hat{\boldsymbol{e}}_z+RdT\hat{\boldsymbol{e}}_z-Rn\phi\hat{\boldsymbol{e}}_z+\sqrt{Ta}\left(\boldsymbol{u}_D\times\hat{\boldsymbol{e}}_z\right), \tag{11}$$

$$\frac{\partial T}{\partial t}+\boldsymbol{u}_D\cdot\nabla T=\frac{\partial^2 T}{\partial z^2}+\zeta\nabla_H^2 T+\frac{N_B}{Ln}\nabla\phi\cdot\nabla T+\frac{N_A N_B}{Ln}\nabla T\cdot\nabla T+Q, \tag{12}$$

$$\frac{\partial\phi}{\sigma\partial t}+\frac{1}{\varepsilon}\boldsymbol{u}_D\cdot\nabla\phi=\frac{1}{Ln}\nabla^2\phi+\frac{N_A}{Ln}\nabla^2 T, \tag{13}$$

with boundary condition as

$$w=0,\frac{\partial w}{\partial z}+\beta_1\frac{\partial^2 w}{\partial z^2}=0,T=1,\phi=0 \text{ at } z=0, \tag{14}$$

$$w=0,\frac{\partial w}{\partial z}-\beta_2\frac{\partial^2 w}{\partial z^2}=0,T=0,\phi=1 \text{ at } z=1, \tag{15}$$

where $Da=\frac{K_V\mu}{\mu L^2}$ define as the Darcy number, $\Pr=\frac{\mu\varepsilon^2L^2}{\kappa_v\rho_f K_V}$ define as the Darcy-Prandtl number, $\boldsymbol{u}_a=\left[\frac{u}{\xi},\frac{v}{\xi},w\right]$ is the anisotropic modified velocity vector, $\hat{\boldsymbol{e}}_z=(0,0,1)$ is the unit vector in the *z*-direction, $Rd=\frac{\rho_f g\alpha_T K_V L\Delta T^*}{\mu\kappa_v}$ where is the thermal Darcy-Rayleigh number, $Ln=\frac{\kappa_v}{D_B}$ is the Lewis number, $Rm=\frac{\left[\rho_p\phi_l^*+\rho_f\left(1-\phi_l^*\right)\right]gK_VL}{\mu\kappa_v}$ is the basic density Rayleigh number, $Rn=\frac{\left(\rho_p-\rho_f\right)\left(\phi_u^*-\phi_l^*\right)gK_VL}{\mu\kappa_v}$ is the concentration Darcy-Rayleigh number, $Ta=\frac{4\Omega^{*2}\tilde{K}_V^2\rho_f^2L^2}{\mu^2\varepsilon^2}$ is the porous media related Taylor number, $N_B=\frac{\varepsilon(\rho c)_p}{(\rho c)_f}\left(\phi_u^*-\phi_l^*\right)$ is the modified particle-density increment, $N_A=\frac{D_T\Delta T^*}{D_BT_u^*\left(\phi_u^*-\phi_l^*\right)}$ is the modified density ratio, $\xi=\frac{\tilde{K}_H}{\tilde{K}_V}$ is the mechanical anisotropy parameter, $\zeta=\frac{\tilde{\kappa}_{mH}}{\tilde{\kappa}_{mV}}$ is the thermal anisotropy parameter and $Q=\frac{Q_0^*L^2}{2\kappa_v(\rho c)_f\Delta T^*}$ represents the dimensionless heat source strength.

In the quiescent basic state, the temperature and volumetric fraction of nanoparticles vary only in the vertical *z*-direction and satisfy the following equations:

$$-\frac{dp_b}{dz}-Rm+RdT_b-Rn\phi_b=0, \tag{16}$$

$$\frac{d^2T_b}{dz^2}+\frac{N_B}{Ln}\frac{dT_b}{dz}\frac{d\phi_b}{dz}+\frac{N_AN_B}{Ln}\left(\frac{dT_b}{dz}\right)^2+Q=0, \tag{17}$$

$$N_A\frac{d^2T_b}{dz^2}+\frac{d^2\phi_b}{dz^2}=0. \tag{18}$$

The above equations are solved subject to the boundary conditions:

$$\begin{aligned}&T_b(0)=1,\phi_b(0)=0 \text{ at } z=0,\\&T_b(1)=0,\phi_b(1)=1 \text{ at } z=1.\end{aligned} \tag{19}$$

Integrating Eq. (18) with respect to *z* and using the boundary condition Eq. (19), we get

$$\phi_b = -N_A T_b + \left(1 - N_A\right) z + N_A. \tag{20}$$

Using Eq. (20) in Eq. (17), we obtain

$$\frac{d^2 T_b}{dz^2} + \frac{\left(1 - N_A\right) N_B}{Ln} \frac{dT_b}{dz} + Q = 0. \tag{21}$$

On integrating Eq. (21) with respect to z twice and using the boundary conditions Eq. (19), we get

$$\begin{aligned} T_b\left(z\right) = {} & \frac{e^{\frac{\left(-1+N_A\right)N_B}{Ln}} \left[-N_B\left(-1+N_A\right) - LnQ\right] - LnQ\left(-1+z\right)}{\left(1+e^{\frac{\left(-1+N_A\right)N_B}{Ln}}\right) N_B\left(-1+N_A\right)} + \\ & \frac{e^{\frac{\left(-1+N_A\right)N_B}{Ln}} \left[N_B\left(-1+N_A\right) + LnQz\right]}{\left(1+e^{\frac{\left(-1+N_A\right)N_B}{Ln}}\right) N_B\left(-1+N_A\right)}, \end{aligned} \tag{22}$$

$$\begin{aligned} \phi_b\left(z\right) = {} & z + \frac{\left[e^{\frac{\left(-1+N_A\right)N_B}{Ln}}\right] \left[N_B\left(-1+N_A\right) + LnQ\right] N_A}{\left(1+e^{\frac{\left(-1+N_A\right)N_B}{Ln}}\right) N_B\left(-1+N_A\right)} + \\ & \frac{\left[z - ze^{\frac{\left(-1+N_A\right)N_B}{Ln}}\right] \left[N_B\left(-1+N_A\right) + LnQ\right] N_A}{\left(1+e^{\frac{\left(-1+N_A\right)N_B}{Ln}}\right) N_B\left(-1+N_A\right)}, \end{aligned} \tag{23}$$

According to Buongiorno [1], for most of the nanofluids, $N_A \approx 1$ to 10, $Ln \approx 10^2$ to 10^3, $N_B \approx 10^{-4}$ to 10^{-2}, and consequently $\varepsilon = \dfrac{\left(N_A - 1\right) N_B}{Ln}$ is very small of order 10^{-7} to 10^{-4}. Hence, expanding $T_b\left(z\right)$ and $\phi_b\left(z\right)$ in power series of ε and retaining up to the first-order terms we have,

$$T_b\left(z\right) = \frac{1}{2}\left(2 - 2z + Qz - Qz^2\right) + \frac{1}{12}\left(6z - Qz - 6z^2 + 3Qz^2 - 2Qz^3\right)\varepsilon + \ldots, \tag{24}$$

$$\phi_b\left(z\right) = \left(z - \frac{N_A Qz}{2} + \frac{N_A Qz^2}{2}\right) + \frac{1}{12}\left(-6N_A z + N_A Qz + 6N_A z^2 - 3N_A Qz^2 + 2N_A Qz^3\right)\varepsilon + \ldots, \tag{25}$$

Here $\varepsilon \approx 10^{-7}$ to 10^{-4}, as compared to $\left[\frac{1}{2}\left(2-2z+Qz-Qz^2\right)\right] \approx 10^0$ or $\left(z-\frac{N_A Qz}{2}+\frac{N_A Qz^2}{2}\right) \approx 10^0$, the zeroth order terms are dominant in both $T_b(z)$ and $\phi_b(z)$, hence approximately, we proceed with

$$T_b(z)=\frac{1}{2}\left(2-2z+Qz-Qz^2\right), \tag{26}$$

$$\phi_b(z)=\left(z-\frac{N_A Qz}{2}+\frac{N_A Qz^2}{2}\right), \tag{27}$$

Which demonstrate quadratic distribution in z.

Suppose that the basic state is disturbed by an infinitesimal thermal perturbation. We now superimpose perturbations on the basic solution. We write:

$$(u,v,w,p,T,\phi,\psi)=\left[0,0,0,p_b(z),T_b(z),\phi_b(z),\psi_{b,z}\right]+\left[u',v',w',p',T',\phi',\psi_z'\right]. \tag{28}$$

We substitute Eq. (28) into Eq. (10) – Eq. (13) and linearize them by neglecting the products of primed quantities and obtain:

$$\nabla\cdot\boldsymbol{u}_D'=0, \tag{29}$$

$$\frac{Da}{\mathrm{Pr}}\frac{\partial \boldsymbol{u}_D'}{\partial t}=-\nabla p'+Da\nabla^2\boldsymbol{u}_D'-\boldsymbol{u}_a'+RdT'\hat{\boldsymbol{e}}_z-Rn\phi'\hat{\boldsymbol{e}}_z-\sqrt{Ta}\left(\boldsymbol{u}_D'\times\hat{\boldsymbol{e}}_z\right), \tag{30}$$

$$\frac{\partial T'}{\partial t}-w'\frac{\partial T_b}{\partial t}=\frac{\partial^2 T'}{\partial z^2}+\zeta\nabla_H^2 T'+\frac{N_B}{Ln}\frac{\partial\phi_b}{\partial z}\frac{\partial T'}{\partial z}-2\frac{N_A N_B}{Ln}\frac{\partial T_b}{\partial z}\frac{\partial T'}{\partial z}-\frac{N_B}{Ln}\frac{\partial T_b}{\partial z}\frac{\partial\phi'}{\partial z}, \tag{31}$$

$$\frac{\partial\phi'}{\sigma\partial t}+\frac{1}{\varepsilon}\frac{\partial\phi_b}{\partial z}w'=\frac{1}{Ln}\nabla^2\phi'+\frac{N_A}{Ln}\nabla^2 T', \tag{32}$$

Where $T_b=\frac{1}{2}\left(2-2z+Qz-Qz^2\right)$ and $\phi_b=2z-N_A Qz+N_A Qz^2$.

Taking operation of the $\hat{\boldsymbol{e}}_z\cdot\mathrm{curl}(\nabla\times)$ on Eq. (30), we get:

$$\left[Da\nabla^2-\frac{Da}{\mathrm{Pr}}\frac{\partial}{\partial t}+\frac{1}{\xi}\right]\boldsymbol{\psi}'+Rd\nabla\times\left(T'\hat{\boldsymbol{e}}_z\right)-Rn\nabla\times\left(\phi'\hat{\boldsymbol{e}}_z\right)-\sqrt{Ta}\nabla\times\left(\boldsymbol{u}_D'\times\hat{\boldsymbol{e}}_z\right)=0, \tag{33}$$

and retaining the *z*-component, we obtain:

$$\left[Da\nabla^2-\frac{Da}{\mathrm{Pr}}\frac{\partial}{\partial t}+\frac{1}{\xi}\right]\psi_z'-\sqrt{Ta}\frac{\partial w'}{\partial z}=0. \tag{34}$$

Operating on Eq. (33) with curl twice, together with curl identity and the continuity Eq. (29). Then, retaining the *z*-component, and simplified with Eq. (34), we obtain:

$$\left[Da\nabla^2 - \frac{Da}{\Pr}\frac{\partial}{\partial t} + \frac{1}{\xi} \right] \left[\left\{ Da\nabla^4 - \frac{Da\nabla^2}{\Pr}\frac{\partial}{\partial t} + \left(\nabla_H^2 + \frac{\partial^2}{\xi \partial z^2} \right) \right\} w' + Rd\nabla_H^2 T' - Rn\nabla_H^2 \phi' \right] - Ta\frac{\partial^2 w'}{\partial z^2} = 0. \quad (35)$$

The normal mode expansion of the dependent variable is assumed in the form:

$$\left(w', T', \phi'\right) = \left[W(z), \Theta(z), \Phi(z) \right] e^{\left[i\left(a_x x + a_y y\right) + st \right]}, \quad (36)$$

Substitute the normal mode expansion of Eq. (36) into Eq. (31), Eq. (32) and Eq. (35), we obtain:

$$\left[Da\left(D^2 - a^2\right) + \frac{1}{\xi} \right] \left[\left\{ Da\left(D^2 - a^2\right)^2 + \frac{1}{\xi} D^2 - a^2 \right\} W - a^2 Rd\Theta + a^2 Rn\Phi \right] + TaD^2 W = 0, \quad (37)$$

$$\left[D^2 - \zeta a^2 + \frac{N_A N_B}{Ln}\left(-2 + Q - 2Qz\right) + \frac{N_B}{Ln}\left(1 - \frac{N_A Q}{2} + N_A Qz\right) D \right] \Theta - \frac{\left(Q - 2 - 2Qz\right)}{2} W - \frac{N_B}{2Ln}\left(Q - 2 - 2Qz\right) D\Phi = 0, \quad (38)$$

$$\frac{-1}{\varepsilon}\left(1 - \frac{N_A Q}{2} + N_A Qz\right) W - \frac{N_A}{Ln}\left(D^2 - a^2\right)\Theta - \frac{1}{Ln}\left(D^2 - a^2\right)\Phi = 0, \quad (39)$$

Where $a = \sqrt{a_x^2 + a_y^2}$ is the wavenumber, and $D = \frac{d}{dz}$.

Following the proportional feedback control [26], the continuously distributed actuators and sensors are arranged in a way that for every sensor, there is an actuator positioned directly beneath it. The determination of a control, $q(t)$ can be accomplished using the proportional-integral-differential (PID) controller of the form:

$$q(t) = r + K\left[e(t) \right], \quad (40)$$

where *r* is the calibration of the control, $e(t) = \hat{m}(t) + m(t)$ an error or deviation from the measurement, $\hat{m}(t)$, from some desired reference value, $m(t)$, *K* is the scalar controller gain where $K = K_P + K_D\frac{d}{dt} + K_L\int_0^t dt$, K_P is the proportional gain, K_D is the differential gain and K_L is the integral gain.

Based on Eq. (40), for one sensor plane and proportional feedback control, the actuator modifies the heated surface temperature using a proportional relation between the upper, $z = 1$ and the lower, $z = 0$, thermal boundaries for the perturbation field

$$T'(x, y, 0, t) = -KT'(x, y, 1, t), \quad (41)$$

Where T' denotes the deviation of the temperature of fluid from its conductive state.

Eq. (37) – Eq. (40) are solved subject to the appropriate boundary conditions. Considering the proportional controller; *K* positioned at the lower boundary of nanofluid layer, we will have:

$$W = DW = \Theta(0) + K\Theta(1) = \Phi = \Psi = D\Psi \quad \text{at} \quad z = 0. \tag{42}$$

We assumed that the upper boundary is non-deformable and insulating to temperature perturbations. The suitable upper boundary conditions are as below.

For lower free and free boundaries

$$\begin{aligned} &W = D^2W = \Theta(0) + K\Theta(1) = \Phi = 0 \quad \text{at} \quad z = 0, \\ &W = D^2W = D\Theta = \Phi = 0 \quad \text{at} \quad z = 1. \end{aligned} \tag{43}$$

For lower rigid and upper free boundaries

$$\begin{aligned} &W = DW = \Theta(0) + K\Theta(1) = \Phi = 0 \quad \text{at} \quad z = 0, \\ &W = D^2W = D\Theta = \Phi = 0 \quad \text{at} \quad z = 1. \end{aligned} \tag{44}$$

For lower rigid and upper rigid boundaries

$$\begin{aligned} &W = DW = \Theta(0) + K\Theta(1) = \Phi = 0 \quad \text{at} \quad z = 0, \\ &W = DW = D\Theta = \Phi = 0 \quad \text{at} \quad z = 1. \end{aligned} \tag{45}$$

The Galerkin type weighted residuals method is applied to find an approximate solution of the system. The variables are written in a series of bases functions:

$$W = \sum_{i=1}^{n} A_i W_i, \Theta = \sum_{i=1}^{n} B_i \Theta_i, \Phi = \sum_{i=1}^{n} C_i \Phi_i, \tag{46}$$

Where A_i, B_i and C_i, are constant and the bases functions W_i, Θ_i and Φ_i where $i = 1, 2, 3, \ldots$, will be chosen corresponding to the free-free, rigid-free and rigid-rigid lower-upper boundary conditions. Substitute Eq. (46) into Eq. (37) - Eq. (39) and make the expressions on the left-hand side of those equations (the residuals) orthogonal to the trial functions, thereby obtaining a system of *3N* linear algebraic equations in the *3N* unknowns. The vanishing of the determinant of the coefficients produces the eigenvalue equation for the system. One can regard *Rd* as the eigenvalue solution; thus, *Rd* is found in terms of the other parameters and solve by Maple software.

3. Results

Thermogravitational convection of Darcy-Brinkman nanofluids layer saturated in a rotating anisotropic porous medium with feedback control and internal heat source is investigated. The nanofluid model integrates the influences of Brownian motion and thermophoresis mechanisms, whereas the Brinkman model is considered for porous medium. Three distinct lower-upper boundary

conditions are taken into account: both boundaries being free (free-free), both boundaries being rigid (rigid-rigid), and lower boundary being rigid while the upper is free (rigid-free). The numerical solution to the resulting generalized eigenvalue problem is obtained using the Galerkin method. The parameters values are selected based on the recommendations made by Yadav *et al.,* [6] and Agarwal *et al.,* [21]. The parameters are fixed with *Ta* = 500, *K* = 5, $\varepsilon = 0.6$, $\xi = 0.8$, $\zeta = 0.6$, $N_A = 1$, $N_B = 0.01$, *Rn* = 2, *Ln* = 100, *Q* = 0.5 with *Da* = 0.2 and 0.9 for the configuration of Darcy-Rayleigh number, *Rd* versus wavenumber, *a* in Figures 2-10. As for the critical Darcy-Rayleigh number, Rd_c versus the various of effects is plotted in Figures 11-16 with parameters fixed at *Ta* = 500, *K* = 5, $\varepsilon = 0.6$, $\xi = 0.8$, $\zeta = 0.6$, $N_A = 1$, $N_B = 0.01$, *Rn* = 2, *Ln* = 100, *Q* = 0.5 and *Da* = 0.8 except for the varying parameters.

We conducted test computations and compared our results with those of Yadav *et al.,* [6] and, Char and Chiang [29], specifically for the limiting case of nanofluids (regular fluids) without porous media. The critical Darcy-Rayleigh number, Rd_c for the rigid-free and free-free boundary conditions were compared, and the results are presented in Tables 1-3. The tables clearly demonstrate that our results align well with the findings reported by Yadav *et al.,* [6], and Char and Chiang [29], thereby confirming the accuracy of our analysis.

Table 1
Comparisons of critical Darcy-Rayleigh number, Rd_c for different values of *Q* with Char and Chiang [29] and Yadav *et al.,* [6] for regular fluids in the absence of porous media in rigid-rigid boundary conditions

Q	Rd_c		
	Char Chiang [29]	Yadav *et al.,* [6]	Present Study
0	1707.85	1707.75	1707.85
1	1704.61	1704.52	1705.41
2	1695.04	1694.94	1702.97
10	1463.05	1462.86	1463.13
20	1118.66	1118.45	1118.35

Table 2
Comparisons of critical Darcy-Rayleigh number, Rd_c for different values of *Q* with Char and Chiang [29] and Yadav *et al.,* [6] for regular fluids in the absence of porous media in rigid-free boundary conditions

Q	Rd_c		
	Char Chiang [29]	Yadav *et al.,* [6]	Present Study
0	1100.65	1100.64	1100.65
1	1055.58	1055.57	1055.16
2	1011.44	1011.43	1011.43
10	725.60	725.60	725.59
20	517.87	517.83	517.73

Table 3
Comparisons of critical Darcy-Rayleigh number, Rd_c for different values of Q with Yadav *et al.,* [6] for regular fluids in the absence of porous media in free-free boundary conditions

	Rd_c	
Q	Yadav *et al.,* [6]	Present Study
0	657.51	657.59
1	656.69	656.59
2	654.25	654.26
10	589.46	589.53
20	473.46	473.67

Figure 2 illustrates the plot of Darcy-Rayleigh number, *Rd* and the corresponding wavenumber, *a* for selected values of feedback control *K* = 5 and 7. Two values of Darcy number, *Da* = 0.2 and 0.9 are considered. Increasing the feedback control *K* causes the marginal stability curves to shift upwards, indicating that the controller stabilizes the motionless state for all wavenumbers. This phenomenon occurs as the sensors detect the deviations from the conductive state of the nanofluids layer, prompting the actuators to suppress any disturbances [25]. Simultaneously, the Darcy-Rayleigh number, *Rd* increases with higher values of the Darcy number *Da*. This observation suggests that the Darcy number, *Da* has a delaying effect on the onset of convection within the nanofluids layer saturated in porous medium, as previously indicated [2, 3, 6]. In the work analysed by Kuznetsov and Nield [3], which explored the thermal instability of nanofluids layer saturated in a porous medium using the Brinkman model, the expression for the thermal Darcy-Rayleigh number, *Rd* is provided by

$$Rd + \left(N_A + \frac{Ln}{\varepsilon} \right) Rn = \frac{\left(\pi^2 + a^2 \right)^2 + Da\left(\pi^2 + a^2 \right)^2}{a^2}. \tag{47}$$

Based on their expression of *Rd* in Eq. (47), we performed an analysis to investigate the influence of the Darcy number parameter. Increasing the Darcy number results in a higher Darcy-Rayleigh number *Rd* and stabilizes the system [2, 3, 6]. These findings validate the accuracy of our results. Notably, the effects of both *K* and *Da* are significant in slowing down the onset of convective instability in the system. Furthermore, it is noteworthy that the rigid-rigid boundary conditions exhibit the most substantial stability compared to rigid-free and free-free boundaries.

Figure 3 depicts the relationship between the Taylor number, *Ta* = 500 and 700 for two values of Darcy number, *Da* = 0.2 and 0.9 in the plot of Darcy-Rayleigh number, *Rd* versus wavenumber, *a* respectively. As the Taylor number, *Ta* increases, the Darcy-Rayleigh number, *Rd* also rises. This behaviour indicates that the Coriolis force resulting from the rotation inhibits the onset of convection within nanofluids layer. The rotational motion causes the nanofluids to move more vigorously in the horizontal plane due to the vorticity introduced by the rotation mechanism. Consequently, the velocity of the nanofluids in the vertical plane decreases, resulting in a reduction in thermal convection.

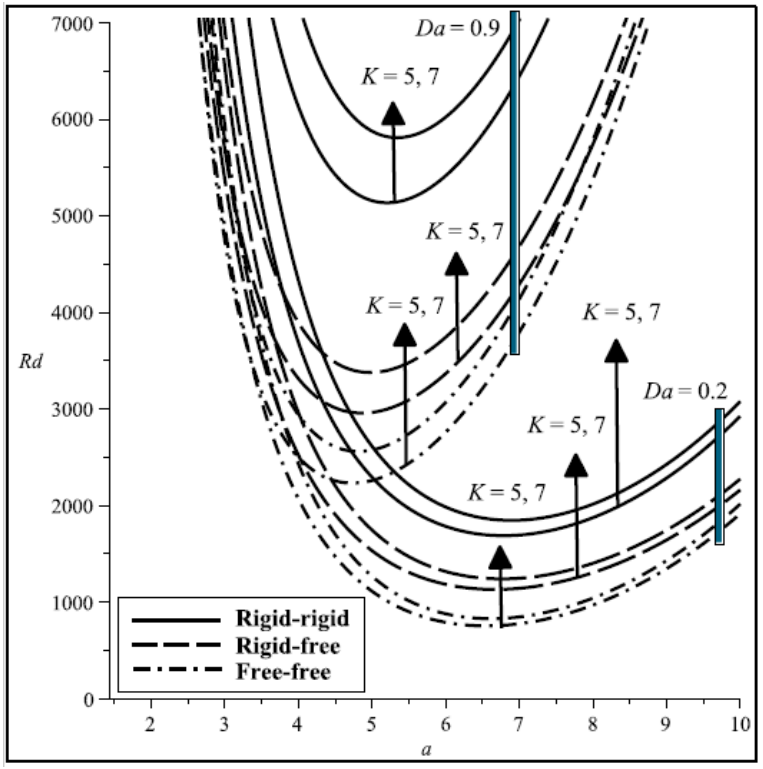

Fig. 2. Variation of *K* on *Rd* against *a* for different values of *Da*

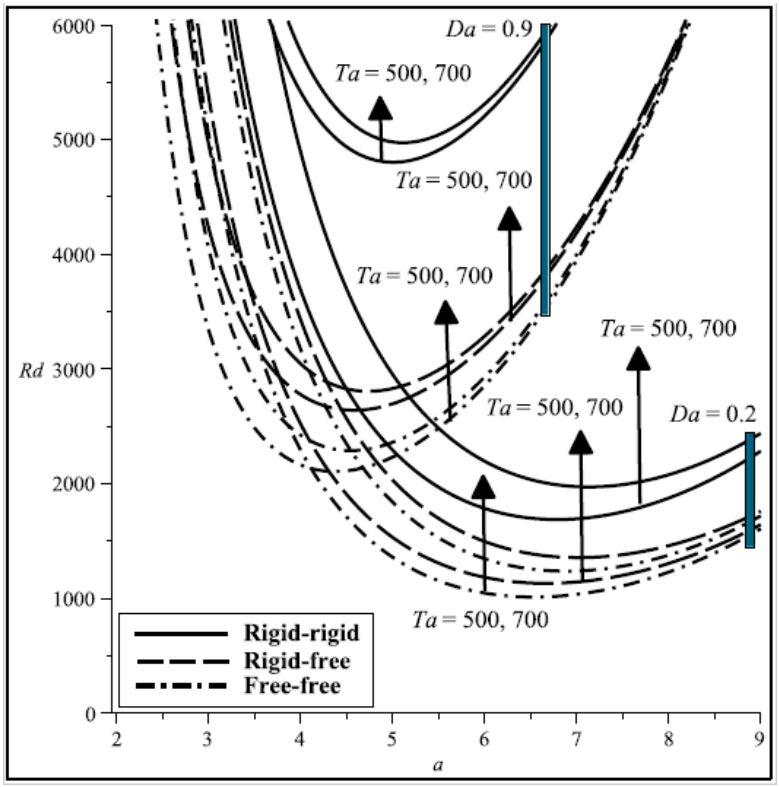

Fig. 3. Variation of *Ta* on *Rd* against *a* for different values of *Da*

Figure 4 illustrates the relationship between the Darcy-Rayleigh number, *Rd* and the wavenumber, *a* for different values of the mechanical anisotropy parameter $\xi = 0.3$ and 0.8 for two values of Darcy number, *Da* = 0.2 and 0.9. It is observed that increasing the mechanical anisotropy parameter, ξ leads to a corresponding increase in the value of *Rd*, indicating a stabilizing effect on

thermal instability [21]. Conversely, decreasing the value of ξ exhibits the opposite trend. Briefly, permeability is defined as the ability of a porous material to transmit fluids. Considering the definition of the mechanical anisotropy parameter, an increase in the mechanical anisotropy parameter ξ causes the permeability $\tilde{K}_H$ in the *x*-direction to increase or the permeability in the *z*-direction $\tilde{K}_V$, to decrease. Consequently, it becomes more challenging for nanofluids layer to flow in the *z*-direction, resulting in the onset of convection at a higher Darcy-Rayleigh number, *Rd*. Furthermore, in Figure 5, the effect of the thermal anisotropy parameter $\zeta = 0.5$ and 0.7 for two values of Darcy number, *Da* = 0.2 and 0.9 on the instability is demonstrated. The Darcy-Rayleigh number, *Rd* increases as the thermal anisotropy parameter, ζ increases, indicating that the effect of thermal anisotropy parameter, ζ has a stabilizing effect on the system [21]. According to the definition of the thermal anisotropy parameter, ζ, an increase in ζ leads to an increase in the thermal conductivity, $\tilde{\kappa}_{mH}$ in the *x*-direction increases or a decrease in the thermal conductivity, $\tilde{\kappa}_{mH}$ in the *z*-direction. Consequently, this delay in the onset of convection occurs.

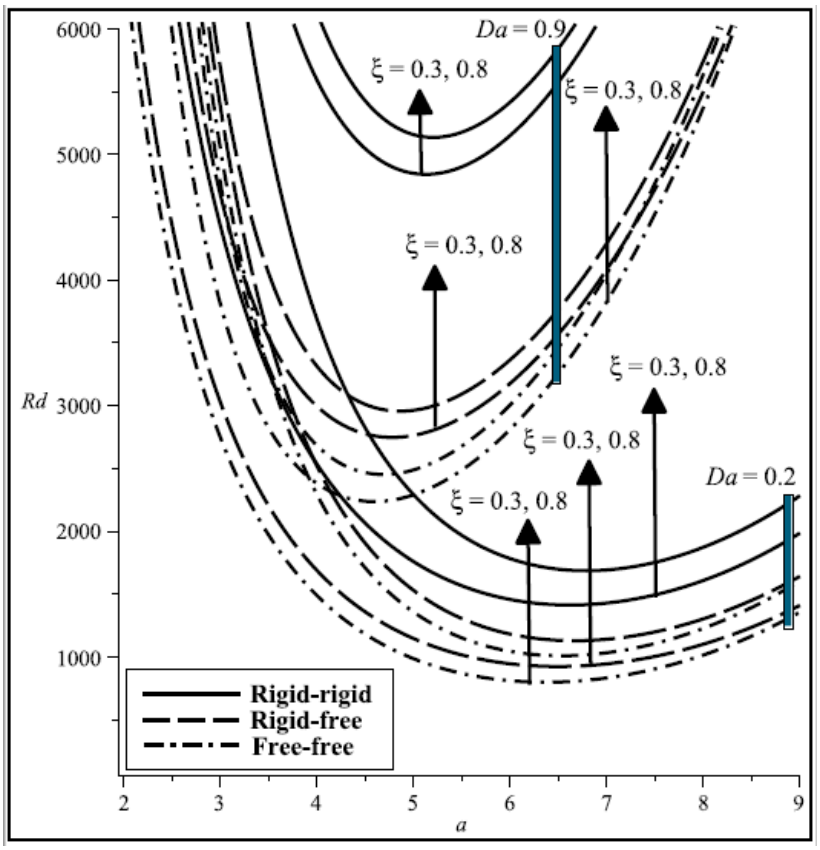

Fig. 4. Variation of ξ on Rd against a for different values of Da

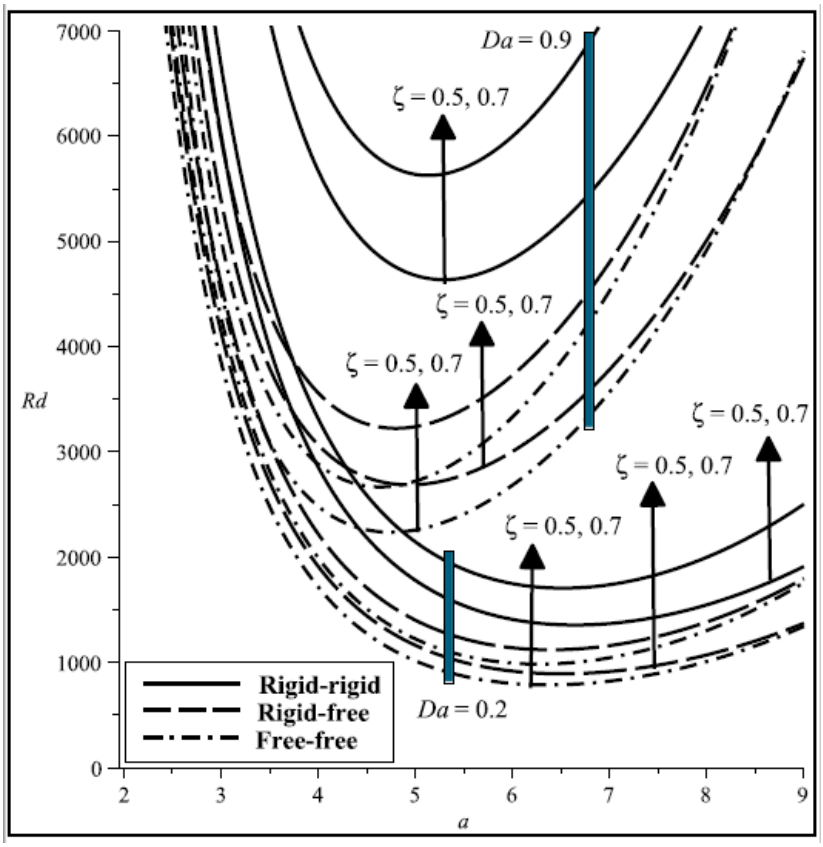

Fig. 5. Variation of ζ on *Rd* against *a* for different values of *Da*

Figure 6 demonstrates the influence of the porosity parameter ε = 0.3 and 0.9 for two values of Darcy number, *Da* = 0.2 and 0.9, on the stationary convection. It is observed that the Darcy-Rayleigh number, *Rd* increases as the porosity parameter ε increases. This indicates that the porosity parameter ε inhibits the onset of Rayleigh-Benard convection and stabilizes the system. It was found that increasing the values of the porosity parameter leads to an increase in the Darcy-Rayleigh number, *Rd*, thus stabilizing the system. Porosity ε in a porous medium is defined as the fraction of the total volume occupied by void spaces. An increase in porosity increases the volume of void spaces, thereby retarding the flow of nanofluids and delaying the onset of Rayleigh-Benard convection. The presence of an internal heat source, *Q* in the system significantly affects its stability of the system. To examine the effect of the internal heat source, *Q* on the criterion for the onset of thermal convection in nanofluids, Figure 7 is plotted for different values of *Q* = 0.5 and 1 when Darcy number, *Da* = 0.2 and 0.9 in three types of boundary conditions. This plot demonstrates that as the strength of the internal heat source *Q* increases, the Darcy-Rayleigh number, *Rd* value decreases. Increasing the internal heat source, *Q* implies an increased energy supply to the system, leading to larger deviations in temperature distributions. These deviations, in turn, enhance disturbances in the nanofluids layer, rendering the system unstable.

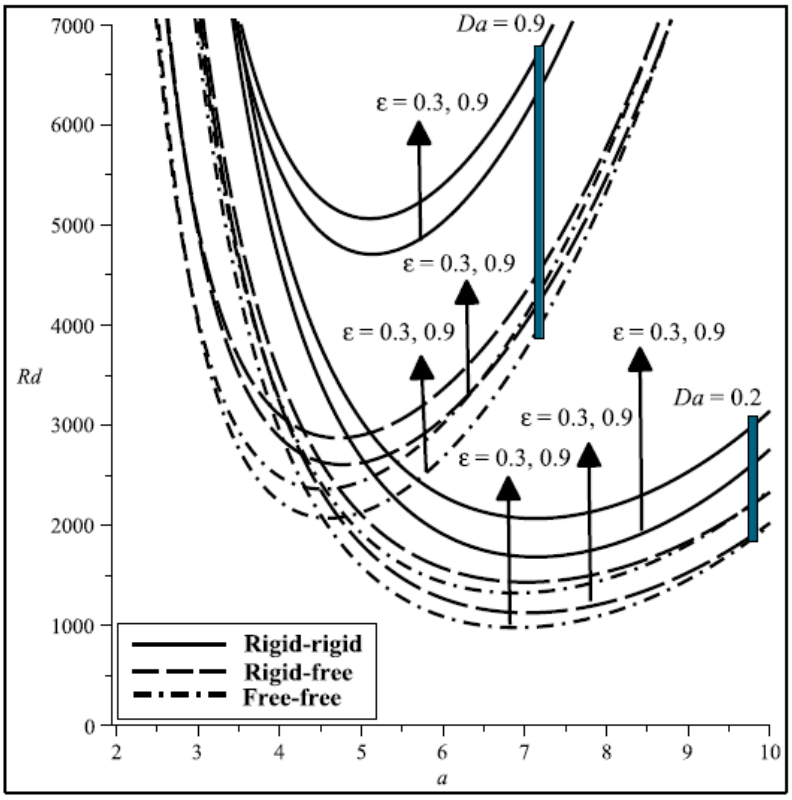

Fig. 6. Variation of ε on *Rd* against *a* for different values of *Da*

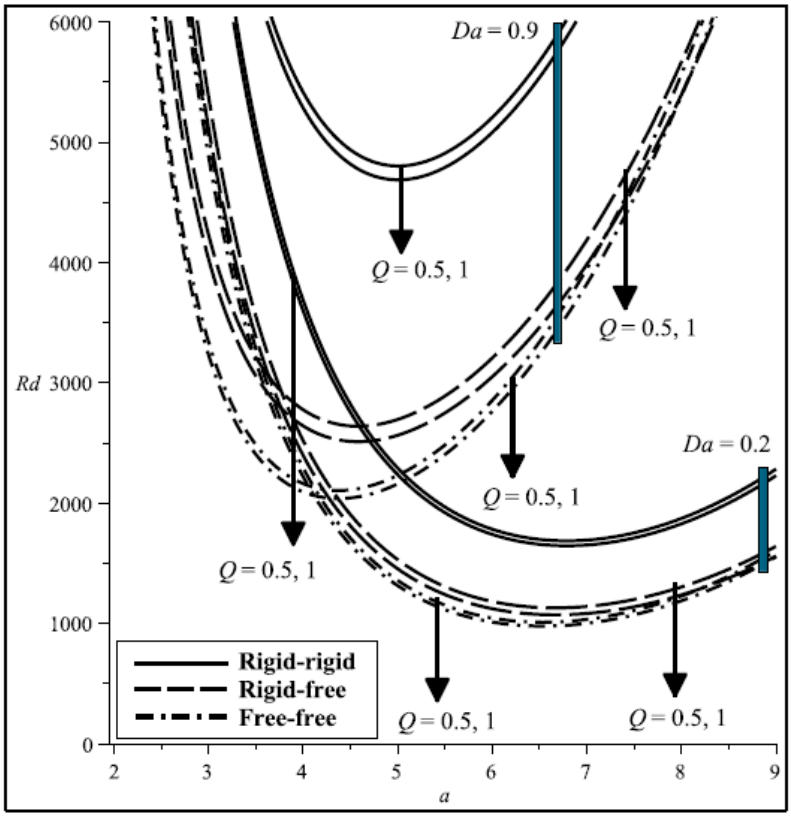

Fig. 7. Variation of *Q* on *Rd* against *a* for different values of *Da*

The effects of the Taylor number, *Ta* on the internal heat source, *Q* = 0.5 and 1 are presented in Figure 8, respectively. It is evident that increasing the Coriolis force due to rotation within nanofluids

layer helps to mitigate the disturbances caused by the internal heat source, *Q*, thereby promoting stability within the nanofluids layer system. Analysing the critical Darcy-Rayleigh number, Rd_c under different boundary conditions, it is observed that the rigid-rigid boundaries consistently exhibit higher values of Rd_c compared to the free-free and rigid-free boundaries.

The graphs of critical Darcy-Rayleigh number, Rd_c against feedback control, *K* for selected values of nanoparticles concentration Rayleigh number, *Rn* = 1 and 3 are depicted in Figure 9, respectively. As previously mentioned, increasing the nanoparticles concentration Rayleigh number, *Rn* monotonically decreases the critical Darcy-Rayleigh number, Rd_c, thereby promoting thermal instability in the system. However, increasing the feedback control, *K* helps to delay the onset of convection induced by the nanoparticles concentration Rayleigh number, *Rn* parameter in the rotating nanofluids layer, thus maintaining system stability.

Meanwhile, Figure 10 displays the variation of the critical Darcy-Rayleigh number, Rd_c as a function of the Darcy number, *Da* for the selected values of porosity ε = 0.2 and 0.8. The results highlight the significant role of porosity, ε and Darcy number, *Da* in stabilizing the system. Finally, the impact of anisotropic parameters on the onset of convection is depicted in Figure 11. The variation of the critical Darcy-Rayleigh number, Rd_c against the thermal anisotropy parameter ζ is presented for selected values of the mechanical anisotropy parameter ξ = 0.4 and 0.8. It is observed that increasing the mechanical anisotropy parameter ξ and thermal anisotropy parameter ζ both contribute to slowing down the onset of convection, thus stabilizing the nanofluids layer system [21].

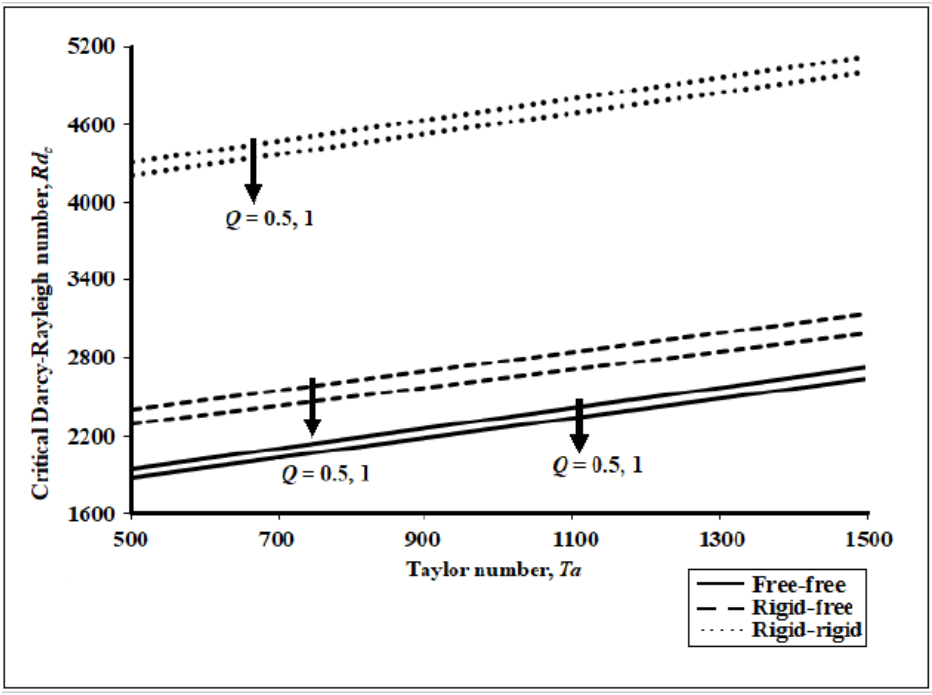

Fig. 8. The plot of Rd_c in the function of *Ta* for selected values of *Q*

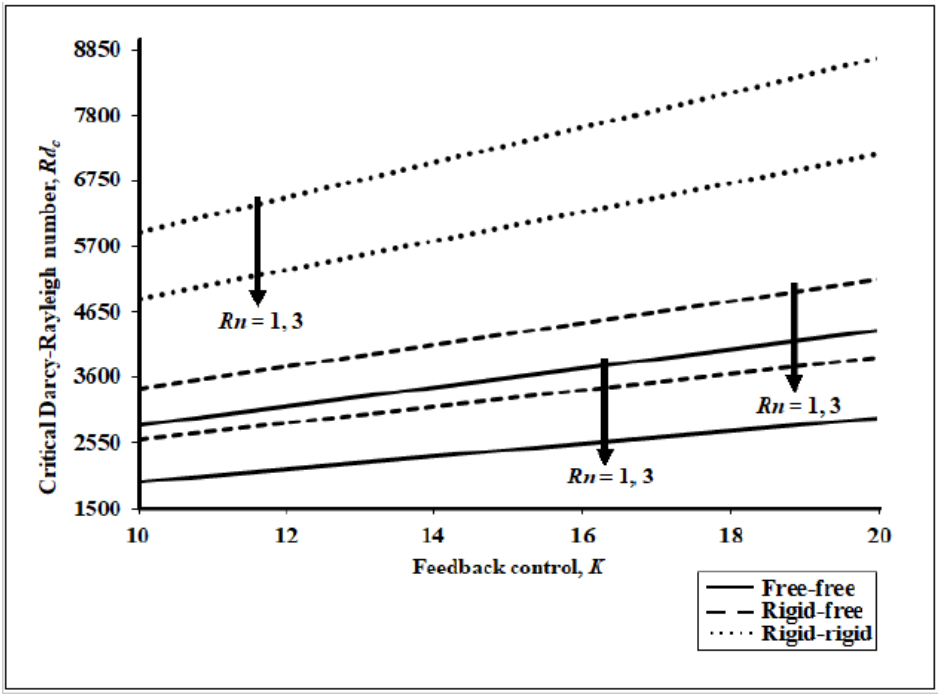

Fig. 9. The plot of Rd_c in the function of K for selected values of Rn

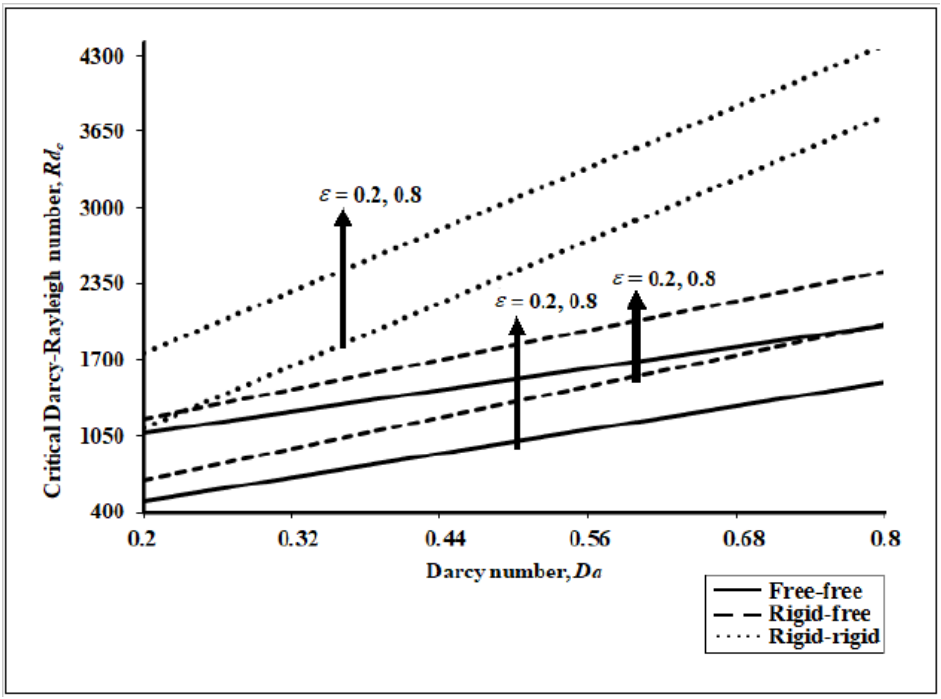

Fig. 10. The plot of Rd_c in the function of Da for selected values of ε

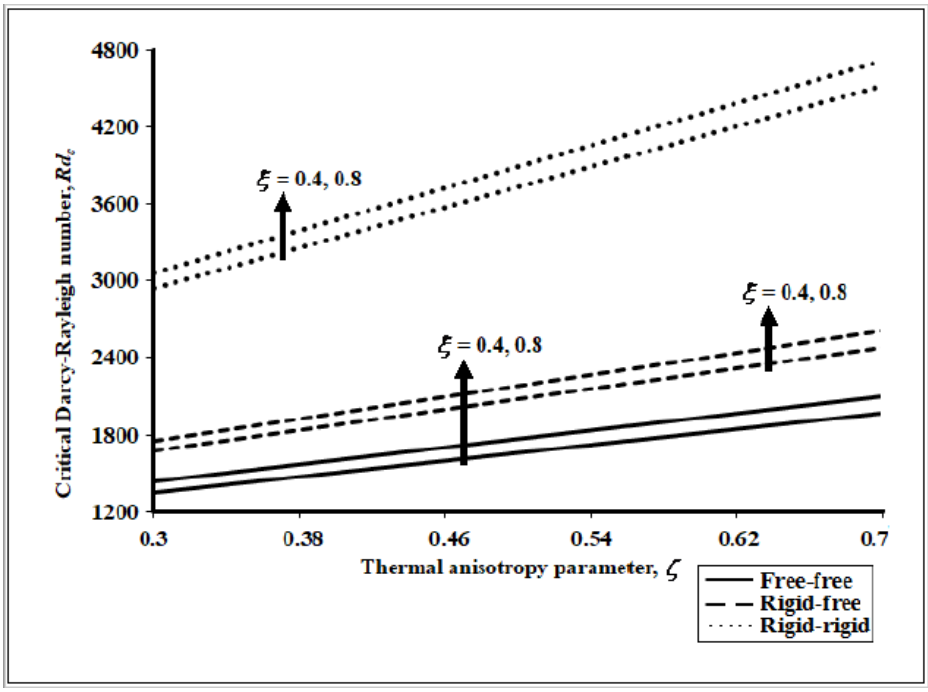

Fig. 11. The plot of Rd_c in the function of ζ for selected values of ξ

4. Conclusions

A theoretical analysis is conducted on the thermogravitational convection of Darcy-Brinkman nanofluids layer saturating in a rotating anisotropic porous medium, considering the effects of feedback control and internal heat source heated from below is analysed theoretically. The model used for nanofluids combines the Brownian motion and thermophoresis mechanism, as proposed by Buongiorno [1]. The Brinkman model is employed to describe the porous medium, considering three different lower-upper boundary combinations: free-free, rigid-free, and rigid-rigid. The linear stability analysis is performed using the normal mode technique, and the resulting eigenvalue problem is numerically solved using the Galerkin technique implemented in Maple software.

The obtained results from the analysis lead to the following conclusions:

i. The implementation effects of feedback control, *K*, Taylor number, *Ta*, Darcy number, *Da*, porosity, ε, mechanical anisotropy parameter, ξ and thermal anisotropy parameter, ζ significantly slows down the Rayleigh-Benard convective instability when their values are increased. Therefore, these factors act as stabilizing agents within the system.

ii. The effects of internal heat source, *Q*, modified diffusivity ratio, N_A, nanofluids Lewis number, *Ln* and nanoparticles concentration Darcy-Rayleigh number, *Rn* enhance the heat transfer mechanism, and act as the destabilizing factors within the system when their values are increased.

iii. Regarding the effect of the modified particles density increment, N_B no visible observation of convective instability is observed. This finding aligns well with the results reported earlier by Shivakumara and Dhananjaya [8] and Yadav *et al.,* [12].

iv. Among the three types of lower-upper boundary conditions, the system exhibits the highest stability when both boundaries are rigid-rigid compared to free-free and rigid-free configurations.

v. Overall, this research contributes practically by improving thermal management in electronics through a better understanding of nanofluids behaviour in porous media under the influence of rotation and heat source. It also has optimizing energy extraction and advancing environmental and industrial processes.

Acknowledgement
This paper is funded by the Universiti Teknologi MARA (UiTM) through the MyRA Research Grant LPHD with grant file number 600-RMC 5/3/GPM (064/2022).

References

[1] Buongiorno, Jacopo. "Convective transport in nanofluids." (2006): 240-250. https://doi.org/10.1115/1.2150834
[2] Nield, D. A., and Andrey V. Kuznetsov. "Thermal instability in a porous medium layer saturated by a nanofluid." *International Journal of Heat and Mass Transfer* 52, no. 25-26 (2009): 5796-5801. https://doi.org/10.1016/j.ijheatmasstransfer.2009.07.023
[3] Kuznetsov, A. V., and DA2599973 Nield. "Thermal instability in a porous medium layer saturated by a nanofluid: Brinkman model." *Transport in Porous Media* 81 (2010): 409-422. https://doi.org/10.1007/s11242-009-9413-2
[4] Chand, Ramesh, and G. C. Rana. "On the onset of thermal convection in rotating nanofluid layer saturating a Darcy–Brinkman porous medium." *International Journal of Heat and Mass Transfer* 55, no. 21-22 (2012): 5417-5424. https://doi.org/10.1016/j.ijheatmasstransfer.2012.04.043
[5] Yu, Wei, and Huaqing Xie. "A review on nanofluids: preparation, stability mechanisms, and applications." *Journal of nanomaterials* 2012 (2012): 1-17. https://doi.org/10.1155/2012/435873
[6] Yadav, Dhananjay, R. Bhargava, and G. S. Agrawal. "Boundary and internal heat source effects on the onset of Darcy–Brinkman convection in a porous layer saturated by nanofluid." *International Journal of Thermal Sciences* 60 (2012): 244-254. https://doi.org/10.1016/j.ijthermalsci.2012.05.011
[7] Goharshadi, E. K., Hossein Ahmadzadeh, Sara Samiee, and Mahboobeh Hadadian. "Nanofluids for heat transfer enhancement-a review." (2013): 1-33. https://doi.org/10.1016/j.ijthermalsci.2012.05.011
[8] Shivakumara, I. S., and M. Dhananjaya. "Penetrative Brinkman convection in an anisotropic porous layer saturated by a nanofluid." *Ain Shams engineering journal* 6, no. 2 (2015): 703-713. https://doi.org/10.1016/j.asej.2014.12.005
[9] Chand, R., G. C. Rana, and S. Kumar. "Variable gravity effects on thermal instability of nanofluid in anisotropic porous medium." *International Journal of Applied Mechanics and Engineering* 18, no. 3 (2013): 631-642. https://doi.org/10.2478/ijame-2013-0038
[10] Namikawa, Tomikazu, Masaki Takashima, and Sadami Matsushita. "The effect of rotation on convective instability induced by surface tension and buoyancy." *Journal of the Physical Society of Japan* 28, no. 5 (1970): 1340-1349. https://doi.org/10.1143/JPSJ.28.1340
[11] Kaddame, A., and G. Lebon. "Bénard-Marangoni convection in a rotating fluid with and without surface deformation." *Applied scientific research* 52 (1994): 295-308. https://doi.org/10.1007/BF00936834
[12] Yadav, Dhananjay, G. S. Agrawal, and R. Bhargava. "Thermal instability of rotating nanofluid layer." *International Journal of Engineering Science* 49, no. 11 (2011): 1171-1184. https://doi.org/10.1016/j.ijengsci.2011.07.002
[13] Yadav, Dhananjay, R. Bhargava, and G. S. Agrawal. "Numerical solution of a thermal instability problem in a rotating nanofluid layer." *International Journal of Heat and Mass Transfer* 63 (2013): 313-322. https://doi.org/10.1016/j.ijheatmasstransfer.2013.04.003
[14] Yadav, Dhananjay, G. S. Agrawal, and Jinho Lee. "Thermal instability in a rotating nanofluid layer: a revised model." *Ain Shams Engineering Journal* 7, no. 1 (2016): 431-440. https://doi.org/10.1016/j.asej.2015.05.005
[15] Qin, Y., and P. N. Kaloni. "Nonlinear stability problem of a rotating porous layer." *Quarterly of applied mathematics* 53, no. 1 (1995): 129-142. https://doi.org/10.1090/qam/1315452
[16] Govender, Saneshan, and Peter Vadasz. *Centrifugal and gravity driven convection in rotating porous media--An analogy with the inclined porous layer*. No. CONF-950828-. American Society of Mechanical Engineers, New York, NY (United States), 1995.
[17] Vadasz, Peter. "Coriolis effect on gravity-driven convection in a rotating porous layer heated from below." *Journal of Fluid Mechanics* 376 (1998): 351-375. https://doi.org/10.1017/S0022112098002961
[18] Govender, S. "Coriolis effect on the linear stability of convection in a porous layer placed far away from the axis of rotation." *Transport in porous media* 51 (2003): 315-326. https://doi.org/10.1023/A:1022360424198

[19] Govender, Saneshan. "Coriolis effect on the stability of centrifugally driven convection in a rotating anisotropic porous layer subjected to gravity." *Transport in porous media* 67 (2007): 219-227. https://doi.org/10.1007/s11242-006-9003-5
[20] Malashetty, M. S., Mahantesh Swamy, and Sridhar Kulkarni. "Thermal convection in a rotating porous layer using a thermal nonequilibrium model." *Physics of Fluids* 19, no. 5 (2007). https://doi.org/10.1063/1.2723155
[21] Agarwal, Shilpi, Beer S. Bhadauria, and P. G. Siddheshwar. "Thermal instability of a nanofluid saturating a rotating anisotropic porous medium." *Special Topics & Reviews in Porous Media: An International Journal* 2, no. 1 (2011). https://doi.org/10.1615/SpecialTopicsRevPorousMedia.v2.i1.60
[22] Tang, Jie, and Haim H. Bau. "Feedback control stabilization of the no-motion state of a fluid confined in a horizontal porous layer heated from below." *Journal of Fluid Mechanics* 257 (1993): 485-505. https://doi.org/10.1017/S0022112093003179
[23] Tang, Jie, and Haim H. Bau. "Stabilization of the no-motion state in Rayleigh-Bénard convection through the use of feedback control." *Physical review letters* 70, no. 12 (1993): 1795. https://doi.org/10.1103/PhysRevLett.70.1795
[24] Howle, Laurens E. "Linear stability analysis of controlled Rayleigh-Bénard convection using shadowgraphic measurement." *Physics of Fluids* 9, no. 11 (1997): 3111-3113. https://doi.org/10.1063/1.869428
[25] Bau, Haim H. "Control of Marangoni–Bénard convection." *International Journal of Heat and Mass Transfer* 42, no. 7 (1999): 1327-1341. https://doi.org/10.1016/S0017-9310(98)00234-8
[26] Bachok, Norfifah, Norihan Arifin, and Fadzilah Ali. "Effects of control on the onset of Marangoni-Benard convection with uniform internal heat generation." *MATEMATIKA: Malaysian Journal of Industrial and Applied Mathematics* (2008): 23-29. https://doi.org/10.11113/matematika.v24.n.219
[27] Siri, Z., Z. Mustafa, and I. Hashim. "Effects of rotation and feedback control on Bénard–Marangoni convection." *International journal of heat and mass transfer* 52, no. 25-26 (2009): 5770-5775. https://doi.org/10.1016/j.ijheatmasstransfer.2009.07.025
[28] Khalid, Izzati Khalidah, Nor Fadzillah Mohd Mokhtar, and Norihan Md Arifin. "Rayleigh-Benard convection in micropolar fluid with feedback control effect." *World Applied Sciences Journal* 21, no. 3 (2013): 112-118. https://doi.org/ 10.5829/idosi.wasj.2013.21.am.21132
[29] Char, Ming-I., and Ko-Ta Chiang. "Stability analysis of Benard-Marangoni convection in fluids with internal heat generation." *Journal of Physics D: Applied Physics* 27, no. 4 (1994): 748. https://doi.org/10.1088/0022-3727/27/4/012
[30] Khalid, Izzati K., Nor Fadzillah M. Mokhtar, and Norihan Md Arifin. "Uniform solution on the effect of internal heat generation on Rayleigh-Benard convection in micropolar fluid." *International Journal of Physical and Mathematical Sciences* 7, no. 3 (2013): 440-445. https://doi.org/10.5281/zenodo.1087912
[31] I. K. Khalid, N. F. M. Mokhtar and N. M. Arifin. "Uniform solution on the combined effect of magnetic field and internal heat generation on Rayleigh-Benard convection in micropolar fluid." *Journal of Heat Transfer* 135, (2013): 1-6. https://doi.org/10.1115/1.4024576
[32] Khalid, Izzati Khalidah, Nor Fadzillah Mohd Mokhtar, Ishak Hashim, Zarina Bibi Ibrahim, and S. S. A. Gani. "Effect of internal heat source on the onset of double-diffusive convection in a rotating nanofluid layer with feedback control strategy." *Advances in Mathematical Physics* 2017 (2017). https://doi.org/10.1155/2017/2789024
[33] Khalid, Izzati Khalidah, Nor Fadzillah Mohd Mokhtar, Zailan Siri, Zarina Bibi Ibrahim, and Siti Salwa Abd Gani. "The effect of magnetic field on Marangoni convection in a nanofluid layer with internal heat source." In *AIP Conference Proceedings*, vol. 1905, no. 1. AIP Publishing, 2017. https://doi.org/10.1063/1.5012166
[34] Khalid, Izzati Khalidah, Nor Fadzillah Mohd Mokhtar, Nur Amirah Bakri, Zailan Siri, Zarina Bibi Ibrahim, and Siti Salwa Abd Gani. "On oscillatory magnetoconvection in a nanofluid layer in the presence of internal heat source and Soret effect." In *AIP Conference Proceedings*, vol. 1905, no. 1. AIP Publishing, 2017. https://doi.org/10.1063/1.5012167
[35] Khalid, Izzati Khalidah, Nor Fadzillah Mohd Mokhtar, Zailan Siri, Zarina Bibi Ibrahim, and Siti Salwa Abd Gani. "Effects of internal heat source and soret on the onset of Rayleigh–Bénard convection in a nanofluid layer." In *AIP Conference Proceedings*, vol. 1974, no. 1. AIP Publishing, 2018. https://doi.org/10.1063/1.5041546
[36] Khalid, I. K., N. F. M. Mokhtar, Z. Siri, Z. B. Ibrahim, and S. S. Abd Gani. "Magnetoconvection on the double-diffusive nanofluids layer subjected to internal heat generation in the presence of Soret and Dufour effects." *Malaysian Journal of Mathematical Sciences* 13, no. 3 (2019): 397-418.
[37] Khalid, Izzati Khalidah, Nor Fadzillah Mohd Mokhtar, and Zarina Bibi Ibrahim. "Rayleigh–Bénard convection in rotating nanofluids layer with feedback control subjected to magnetic field." In *Journal of Physics: Conference Series*, vol. 1366, no. 1, p. 012025. IOP Publishing, 2019. https://doi.org/10.1088/1742-6596/1366/1/012025
[38] Khalid, Izzati Khalidah, Nor Fadzillah Mohd Mokhtar, Zarina Bibi Ibrahim, and Zailan Siri. "Rayleigh–Bénard convection in Maxwell nanofluids layer saturated in a rotating porous medium with feedback control subjected to viscosity and thermal conductivity variations." *Applied Nanoscience* 10 (2020): 3085-3095. https://doi.org/10.1007/s13204-020-01302-4

[39] Khalid, Izzati Khalidah, Nor Fadzillah Mohd Mokhtar, and Zarina Bibi Ibrahim. "Rayleigh-Bénard convection in nanofluids layer saturated in a rotating anisotropic porous medium with feedback control and internal heat source." *CFD Letters* 13, no. 11 (2021): 1-20. https://doi.org/10.37934/cfdl.13.11.120

[40] Khalid, Izzati Khalidah, Nor Fadzillah Mohd Mokhtar, and Zarina Bibi Ibrahim. "Control Effect on Rayleigh-Benard Convection in Rotating Nanofluids Layer with Double-Diffusive Coefficients." *CFD Letters* 14, no. 3 (2022): 79-95. https://doi.org/10.37934/cfdl.14.3.7995

[41] Abidin, Nurul Hafizah Zainal, Nor Fadzillah Mohd Mokhtar, Izzati Khalidah Khalid, and Siti Nur Aisyah Azeman. "Oscillatory Mode of Darcy-Rayleigh Convection in a Viscoelastic Double Diffusive Binary Fluid Layer Saturated Anisotropic Porous Layer." *Journal of Advanced Research in Numerical Heat Transfer* 10, no. 1 (2022): 8-19.

[42] Arasteh, Hossein, Ramin Mashayekhi, Marjan Goodarzi, S. Hossein Motaharpour, Mahidzal Dahari, and Davood Toghraie. "Heat and fluid flow analysis of metal foam embedded in a double-layered sinusoidal heat sink under local thermal non-equilibrium condition using nanofluid." *Journal of Thermal Analysis and Calorimetry* 138 (2019): 1461-1476. https://doi.org/10.1007/s10973-019-08168-x

[43] Toghraie, Davood, Ramin Mashayekhi, Hossein Arasteh, Salman Sheykhi, Mohammadreza Niknejadi, and Ali J. Chamkha. "Two-phase investigation of water-Al2O3 nanofluid in a micro concentric annulus under non-uniform heat flux boundary conditions." *International Journal of Numerical Methods for Heat & Fluid Flow* 30, no. 4 (2019): 1795-1814. https://doi.org/10.1108/HFF-11-2018-0628

[44] He, Wei, Behrooz Ruhani, Davood Toghraie, Niloufar Izadpanahi, Navid Nasajpour Esfahani, Arash Karimipour, and Masoud Afrand. "Using of artificial neural networks (ANNs) to predict the thermal conductivity of zinc oxide–silver (50%–50%)/water hybrid Newtonian nanofluid." *International Communications in Heat and Mass Transfer* 116 (2020): 104645. https://doi.org/10.1016/j.icheatmasstransfer.2020.104645

[45] Boroomandpour, Ahmadreza, Davood Toghraie, and Mohammad Hashemian. "A comprehensive experimental investigation of thermal conductivity of a ternary hybrid nanofluid containing MWCNTs-titania-zinc oxide/water-ethylene glycol (80: 20) as well as binary and mono nanofluids." *Synthetic Metals* 268 (2020): 116501. https://doi.org/10.1016/j.synthmet.2020.116501

[46] Yan, Shu-Rong, Davood Toghraie, Lokman Aziz Abdulkareem, As'ad Alizadeh, Pouya Barnoon, and Masoud Afrand. "The rheological behavior of MWCNTs–ZnO/Water–Ethylene glycol hybrid non-Newtonian nanofluid by using of an experimental investigation." *Journal of Materials Research and Technology* 9, no. 4 (2020): 8401-8406. https://doi.org/10.1016/j.jmrt.2020.05.018

[47] Lakshmi, Deepthi Varagani Venkata, and Srinivasa Raju Rallabandi. "Hall Current and Thermal Radiation Effects on MHD Casson Nanofluid Flow Past in The Presence of Heat Source/Sink, Brownian Motion and Thermophoresis." *Journal of Advanced Research in Fluid Mechanics and Thermal Sciences* 105, no. 2 (2023): 51-67. https://doi.org/10.37934/arfmts.105.2.5167